J Solid State Electrochem (1998) 2: 73–77

ORIGINAL PAPER

Rudolf Holze

Underpotential deposit electrocatalysis of fast redox reactions for electrochemical energy storage systems

Received: 27 May 1997 / Accepted: 29 July 1997

Abstract The electrocatalysis of the $Fe^{3+/2+}$ redox reaction at various electrode/electrolyte solution interfaces in the presence/absence of underpotential deposits of various metals has been investigated by the AC impedance method. Exchange current densities and double layer capacity data were obtained. On this basis, changes in the active surface area of the electrode and catalytic effects of the investigated metals were identified.

Key words Electrocatalysis · Underpotential deposition · Electrode impedance measurements

Introduction

Redox reactions like $Fe^{2+} \rightarrow Fe^{3+} + e^-$ proceeding at metal electrodes or at carbon-based electrode materials in contact with electrolyte solutions have attracted the interest of electrochemists for various reasons. Two particular aspects have stimulated the research reported in this communication:

1. For a few redox reactions an outer-sphere mechanism without any close electrode-redox ion interaction has been claimed. Nevertheless, most reactions seem to involve a close approach of the reacting species involving electronic interactions between the reacting ion and the electrode. Thus, the kinetic data obtained for a given electrode reaction can be related to electronic and other surface properties of the electrode material under investigation.
2. Fast redox reactions can be utilised in electrochemical energy storage devices (redox batteries) wherein two redox reactions proceeding at two electrodes are used to store and retrieve electrical energy (see review in [1]).

The schematic flow diagram of this storage device is depicted in Fig. 1 [2, 3].

The work reported here starts with some experimental observations reported for a system wherein the reaction $Fe^{3+} + Cr^{2+} \leftrightarrow Fe^{2+} + Cr^{3+}$ proceeds at graphitic electrodes. The rather sluggish reactions (expressed as a small exchange current density j_0) can be accelerated considerably by adding small amounts of soluble metal salts containing ions of lead, gold or some other elements. Considering the electrode potentials established at both electrodes under conditions of charge and discharge, the metal ions are deposited at electrode potentials positive to the respective Nernstian electrode potential. These layers are called underpotential deposits (upd). Foreign metals present in an amount of up to two monolayers exert a strong influence upon the electrode reaction with respect to both the electrode reaction mechanism and the electrode kinetics [4–27]. Various modes of catalytic action have been considered:

1. Modification of the electronic structure of the surface resulting in an increased reaction rate
2. Adsorption of oxygen or hydroxide ions involved in the main oxidation reaction of the organic substrate at lower electrode potentials
3. A ''third body effect'' which eliminates the reaction between the primary intermediates and/or adsorbed hydrogen atoms, which otherwise results in the firmly bound adsorbate blocking the electrode surface
4. Inhibition of undesired side reactions
5. Changes in the electrochemical double layer resulting in an increased reactant concentration.

Whereas most of the above effects are operative for electrode reactions involving the oxidation of organic fuels at electrodes for sensors or fuel cells, the first may be effective also for redox reactions. Reports in

Presented at the 3rd Indo-German Seminar on 'Modern Aspects of Electrochemistry', 26 September – 1 October 1996, Bangalore, India

R. Holze
Technische Universität Chemnitz, Institut für Chemie,
D-09107 Chemnitz, Germany
Tel.: +49-371 5311509; Fax: +49-371 5311832;
e-mail: rudolf.holze@chemie.tu-chemnitz.de

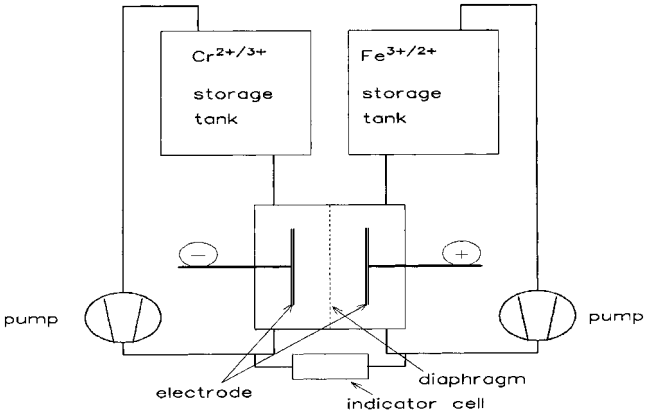

Fig. 1 Schematic flow diagram of a redox battery

the literature have only claimed accelerating or inhibiting effects based on the shifts in current density vs electrode potential curves. Kinetic data, in particular exchange current densities, have not been reported so far. An optimisation of the ionic concentration of the foreign metal ion used for the upd modification has been attempted to a very small extent [24]. In order to quantify the catalytic effects and to get a better understanding of their mechanism on an atomic level, electrode impedance measurements [25], various spectroelectrochemical methods and surface analytical tools were employed. In the present report, results obtained with classical electrochemical methods are described.

Experimental

Carbon disc electrodes embedded in epoxy resin (Araldit D/HY 956, Ciba-Geigy) and polished to a mirror finish with Al_2O_3 (down to 0.3 μm) were manufactured from electrode graphite EH (Sigri), Diabon N (Sigri), ordinary pyrolytic graphite (Ringsdorff) and glassy carbon (Metrohm and Ringsdorff). The working electrode active surface area was 0.282 cm^2 for all graphitic materials and 0.196 cm^2 for glassy carbon.

Electrolyte solutions were prepared from ultrapure water (Seral seralpur pro 90c), 10^{-2} M $(NH_4)_2Fe(SO_4)_2$ and 10^{-2} M $(NH_4)Fe(SO_4)_2$ in 1 M $HClO_4$. For upd modification of platinum electrodes 10^{-3} M $Ni(NO_3)_2$, $Pb(CH_3COO)_2$ and $Cu(CH_3COO)_2$ were added to a solution of 1 M $HClO_4$ only in a separate cell; with carbon electrodes the foreign metal salts were added to the solution containing the redox couple also.

Platinum working electrodes were metal beads (99.99%). A platinum wire served as a counter electrode, and another platinum wire was used as a reference electrode. All measurements (except cyclic voltammograms) were done at the spontaneously established redox potential. Solutions were purged with nitrogen and kept at room temperature (18 °C) during measurements. For cyclic voltammetry and electrode impedance measurements a setup comprising a potentiostat (Solartron 1287), a frequency response analyser (Solartron 1255HF) and an electrochemical cell designed for a.c. measurements. The instruments were interfaced to a PC via an IEEE bus (see Fig. 2). An a.c. amplitude of 10 mV_{pp} was used.

Results and discussion

As a benchmark, the electrode impedance of a platinum electrode in the electrolyte solution was measured. The result is displayed in the complex plane plot in Fig. 3; Fig. 4 shows the corresponding Bode plot. The evaluation is based on a simple equivalent circuit as proposed by Randles [26] and shown in Fig. 5. The parameters of the elements in the equivalent circuit were obtained by a least square fit as described in detail elsewhere [27]. Since the diffusion impedance was not evaluated further, the Nernst impedance (with finite diffusion layer thickness) was used in most cases in a simplified form (Warburg impedance, parameter W). Results are listed in Table 1. The displayed set of results was obtained in independent experiments more than a day apart. They demonstrate convincingly the reproducibility of the method. Underpotential deposit (upd) modification of the platinum electrode was performed in a separate cell by slow cyclic voltammetry. A typical result for modification with lead is shown in Fig. 6.

The charge consumed by the upd amounts to 94 μC cm^{-2}. Assuming a ratio of surface platinum atoms to

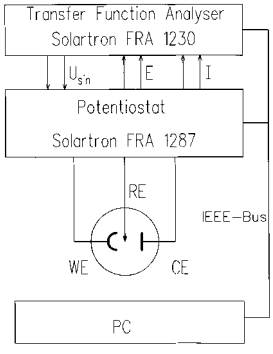

Fig. 2 Schematic diagram of the experimental setup

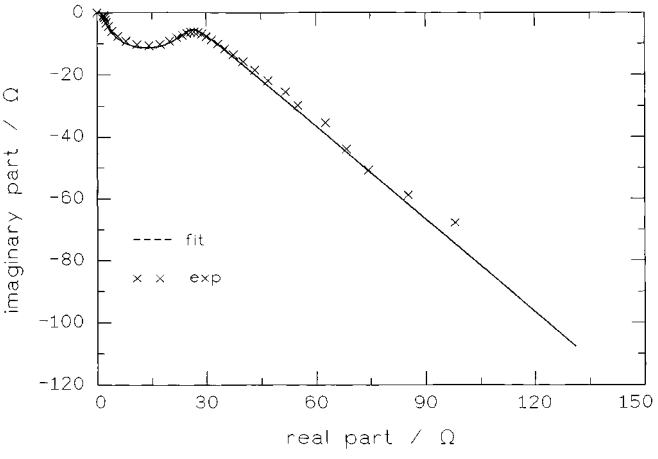

Fig. 3 Electrode impedance of a platinum bead electrode, 10^{-2}M $(NH_4)_2Fe(SO_4)_2$ and 10^{-2} M $(NH_4)Fe(SO_4)_2$ in 1 M $HClO_4$ (complex plane plot)

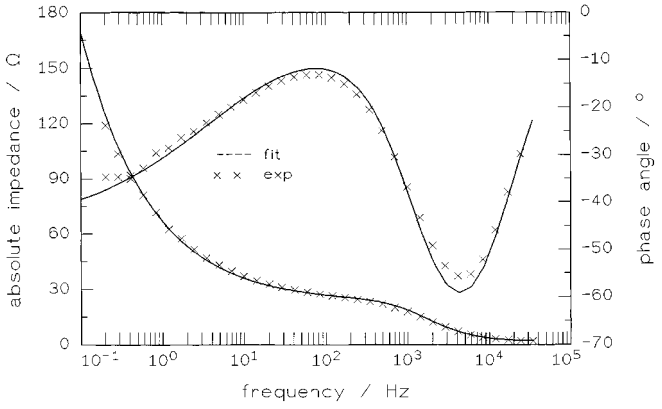

Fig. 4 Electrode impedance of a platinum bead electrode, 10^{-2} M $(NH_4)_2Fe(SO_4)_2$ and 10^{-2} M $(NH_4)Fe(SO_4)_2$ in 1 M $HClO_4$ (Bode plot)

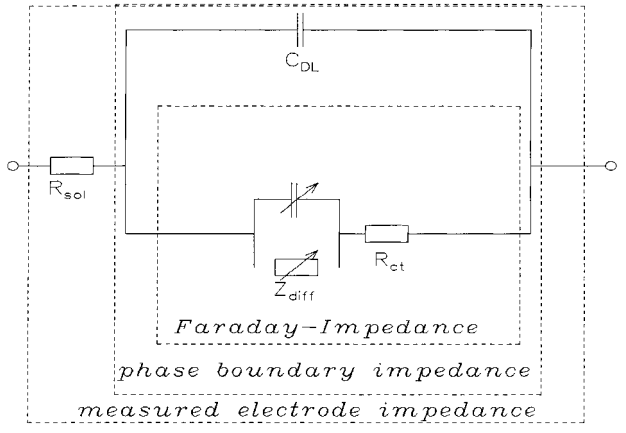

Fig. 5 Equivalent circuit for a platinum bead electrode, 10^{-2} M $(NH_4)_2Fe(SO_4)_2$ and 10^{-2} M $(NH_4)Fe(SO_4)_2$ in 1 M $HClO_4$

Table 1 Kinetic data for a platinum electrode

	Pt (1)	Pt (2)
R_{sol} (Ω)	1.84	1.85
C_{DL} (μF)	5.32	5.32
R_{CT} (Ω)	23.3	23.3
W ($mOhm^{-1}$)	8.18	8.18
j_{00} (A cm^{-2})	0.56	0.56

lead atoms of 1:1 with an atom density for polycrystalline platinum of 1.31×10^{15} cm^{-2} [28], the charge for a monolayer of fully discharged lead atoms would be 419 μC cm^{-2}. The striking discrepancy indicative of a less than full coverage in the present case can be resolved in part based on the observation that no hydrogen adsorption peak was found. This implies a complete blocking of the surface. A similar claim based on a charge of only 86 μC cm^{-2} has been proposed by Pletcher and Solis [6]. Underpotential deposition with nickel results in a less pronounced diagram as displayed in Fig. 7.

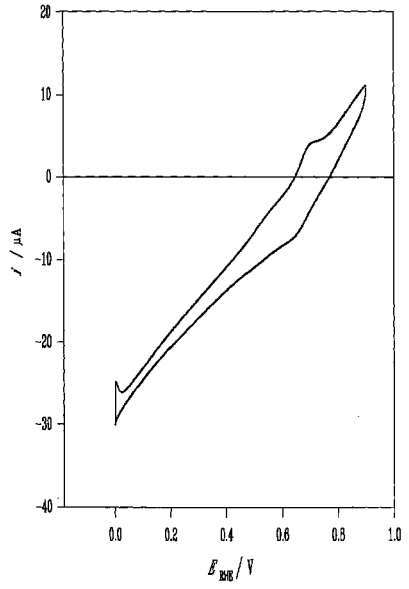

Fig. 6 Cyclic voltammogram (CV) of a platinum bead electrode in a solution of 1 M $HClO_4$ + 1 mM $Pb(CH_3COO)_2$, dE/dt = 10 mV/s

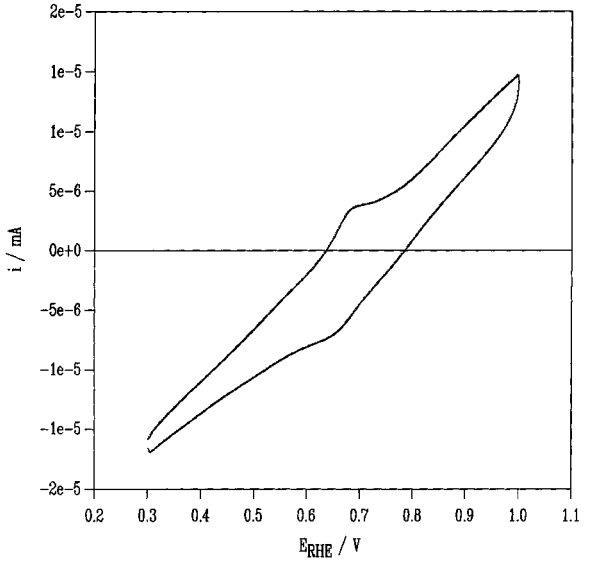

Fig. 7 CV of a platinum bead electrode in a solution of 1 M $HClO_4$ + 1 mM $Ni(NO_3)_2$, dE/dt = 10 mV/s

Again, the full coverage can only be deduced from the absence of the hydrogen adsorption peaks, whereas the charge consumed amounts to 173 μC cm^{-2}, which is considerably less than the amount corresponding to a monolayer. With copper, the charge increased to 270 μC cm^{-2}. Determination of the reported charges is made difficult by the poorly defined peaks. Electrode impedances measured with upd-modified platinum bead electrodes are displayed in Fig. 8; the corresponding kinetic data are collected in Table 2.

In the discussion of catalytic effects, any change of the active surface area has to be taken into account. In the present case, this area is not affected by the upd modification, since the values of C_{DL} are constant.

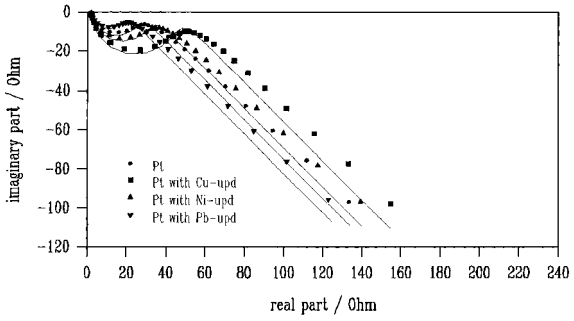

Fig. 8 Electrode impedance plots for an upd-modified platinum bead electrode, 10^{-2} M $(NH_4)_2Fe(SO_4)_2$ and 10^{-2} M $(NH_4)Fe(SO_4)_2$ in 1 M $HClO_4$. *Symbols*: measured values. *Lines*: fitted values, same sequence as measured values (from *left* to *right*: Pt/Pb; Pt; Pt/Ni, Pt/Cu)

Table 2 Impedance parameter of unmodified and upd-modified platinum electrodes

	Pt	Cu-upd	Ni-upd	Pb-upd
R_{sol} (Ω)	1.85	1.84	1.84	1.78
C_{DL} (μF cm^{-2})	27.1	25.2	28.2	28.4
R_{CT} (Ω cm^2)	4.57	7.35	5.72	3.18
W (mOhm^{-1})	8.18	7.99	8.16	8.36
j_{00} (A cm^{-2})	0.56	0.35	0.45	0.81

Thus, with lead an acceleration is observed, whereas nickel and copper seem to have an inhibiting effect.

Corresponding investigations with carbon electrodes turned out to be considerably more difficult. Cyclic voltammograms of graphite EH and glassy carbon before and after extended electrode potential cycling are displayed in Fig. 9.

Impedance data were initially plausible (see Fig. 10), but they turned out to be very irreproducible for all graphitic materials mentioned above. With glassy carbon, the data were fairly reproducible, at least with respect to relative changes of C_{DL} and R_{CT}. A typical set of results is displayed in Fig. 11. Nevertheless, the misfit

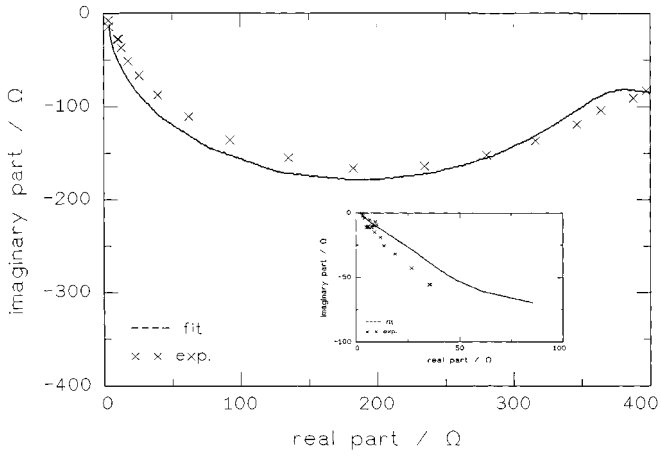

Fig. 10 Electrode impedance plots of graphite EH before and after (*inset*) potential cycling in 10^{-2} M $(NH_4)_2Fe(SO_4)_2$ and 10^{-2} M $(NH_4)Fe(SO_4)_2$ in 1 M $HClO_4$, dE/dt = 100 mV/s

between the shape of the calculated curve and the measured curve indicates a significant weakness of the applied model. Further investigations currently being pursued will reveal whether the corrugated electrode surface or further effects are the cause of this misfit. Because of the still limited reproducibility, only relative changes of R_{CT} could be deduced, as displayed in Fig. 12.

The decrease of R_{CT} corresponding to an increase of j_{00} is indicative of an accelerating effect of the lead adlayer. Since the electrode potential (E_{RHE} = 0.722 V) is considerably positive to the Nernst potential of lead bulk deposition, a upd-modified carbon surface is certainly operative. The increase in C_{DL} nevertheless casts some doubt on the conclusion that only upd catalysis is effective. An increase in the electrode area reflected in an increase in C_{DL} can also cause an increase in the apparent value of j_{00}. Without a precise knowledge of the electrode surface morphology, any conclusion regarding a necessary correction of j_{00} with respect to the true

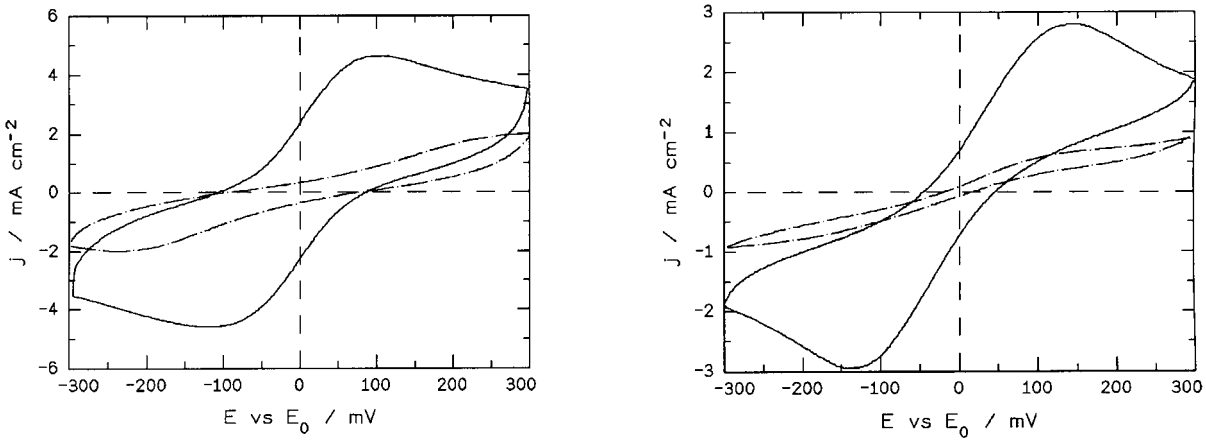

Fig. 9 CVs of graphite EH (*left*) and glassy carbon (*right*) before (-·-·-) and after (—— potential cycling in 10^{-2} M $(NH_4)_2Fe(SO_4)_2$ and 10^{-2} M $(NH_4)Fe(SO_4)_2$ in 1 M $HClO_4$, dE/dt = 100 mV/s

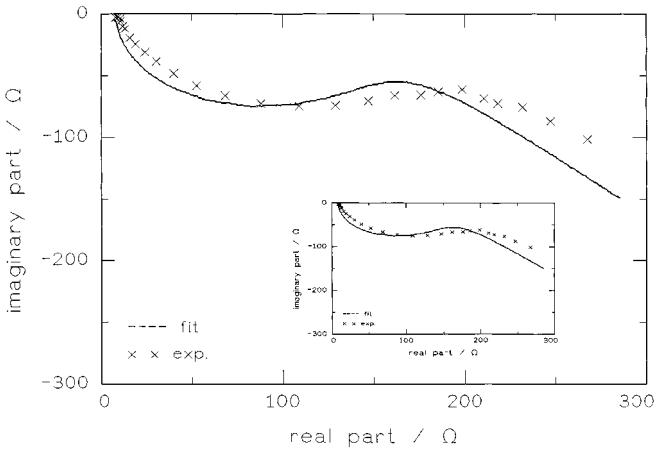

Fig. 11 Electrode impedance plots of glassy carbon before and after (*inset*) potential cycling in 10^{-2} M $(NH_4)_2Fe(SO_4)_2$ and 10^{-2} M $(NH_4)Fe(SO_4)_2$ in 1 M $HClO_4$, dE/dt = 100 mV/s

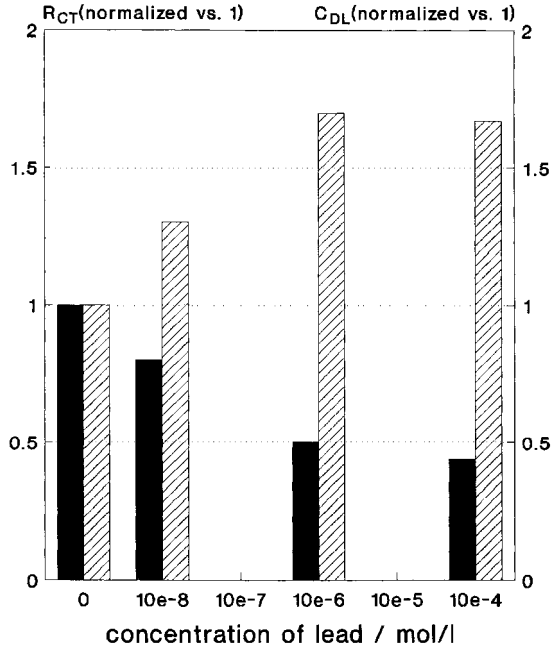

Fig. 12 Relative change of R_{CT} and C_{DL} as a function of the concentration of lead ions

surface area is impossible. A microroughness with typical dimensions in the range of the diffusion layer thickness is known to be of no measurable significance for the obtained value of j_0 [29].

Acknowledgements This report is based on experimental data provided by Stefan Kania, Peter Roland and Frances Taudt. Financial support of this work by the Deutsche Forschungsgemeinschaft, the Fonds der Chemischen Industrie and the Sächsisches Staatsministerium für Wissenschaft und Kunst is gratefully acknowledged.

References

1. Cnobloch H, Nischik H, Pantel K, Ledjeff K, Heinzel A, Reiner A (1988) Siemens Forsch-Entwickl Ber: 17: 270
2. Cnobloch H, Nischik H, Pantel K, Ledjeff K, Heinzel A (1986) Proceedings of Carbon, 4th International Carbon Conference, Baden-Baden, Germany
3. Cnobloch H, Nischik H, Pantel K, Ledjeff K, Heinzel A, Reiner A (1987) Dechema-Monographie 109: 427
4. Adzi RR, Simi DN, Drazi DM (1975) J Electroanal Chem 65: 587
5. Furuya N, Motoo S (1979) J Electroanal Chem 98: 195
6. Pletcher D, Solis V (1982) J Electroanal Chem 131: 309
7. Motoo S, Shibata M (1982) J Electroanal Chem 139: 119
8. Leiva EPM, Giordano MC (1983) J Electrochem Soc 130: 1305
9. Shabrang M, Mizote H, Bruckenstein S (1984) J Electrochem Soc 131: 306
10. Betowska-Brzezinska M, Heitbaum J, Vielstich W (1985) Electrochim Acta 30: 1465
11. Ross PN (1991) Electrochim Acta 36: 2053
12. Fonsaca ITE, Morin AC, Pletcher D (1987) J Electroanal Chem 218: 327
13. Kokkinidis G, Papanastasiou G (1987) J Electroanal Chem 221: 175
14. Clavilier J, Fernandez-Vega A, Feliu JM, Aldaz A (1991) J Electroanal Chem 258: 89
15. Fernandez-Vega A, Feliu JM, Aldaz A, Clavilier J (1991) J Electroanal Chem 305: 229
16. El-Shafei AA, Shabanah HM, Moussa MNH (1993) J Electroanal Chem 362: 159
17. Hartung R, Willsau J, Heitbaum J (1986) J Electroanal Chem 205: 135
18. Betowska-Brzezinska M (1994) J Electroanal Chem Z Phys Chem NF 185: 91
19. Llorca MJ, Herrero E, Feliu JM, Aldaz A (1994) J Electroanal Chem 373: 217
20. Herrero E, Llorca MJ, Feliu JM, Aldaz A (1995) J Electroanal Chem 383: 145
21. Kokkinidis G (1986) J Electroanal Chem 201: 217
22. Adzi RR (1984) In: Gerischer M, Tobias CW (eds) Advances in electrochemistry and electrochemical engineering, Vol. 13. Wiley, New York
23. Parsons R, VanderNoot T (1988) J Electroanal Chem 257: 9
24. Cheng D, Hollax E, Ger Pat DE 3 333 650
25. Holze R (1994) Bull Electrochem 10: 56
26. Randles JEB (1947) Disc Far Soc 1: 11
27. Holze R (1983) Dissertation, University of Bonn
28. Angerstein-Kozlowska H in: Comprehensive treatise of electrochemistry, vol. 9. Plenum, New York, p 24
29. Herrmann J (1983) PhD thesis, University of Bonn